

Research note

## A Study of Catalytic Performance of $\text{Co}_3\text{O}_4$ and Cu-Co Nano Metal Oxides in Combustion of Aromatics

S. A. Hosseini

Department of Applied Chemistry, Faculty of Chemistry, Urmia University, Urmia, Iran

---

### ARTICLE INFO

#### Article history:

Received: 2016-05-26

Accepted: 2016-10-27

#### Keywords:

Nano Spinel

Nano Metal Oxides

Catalytic Combustion

XPS

VOC

Nano Cobaltite

---

### ABSTRACT

Two Cu-Co and  $\text{Co}_3\text{O}_4$  oxides were synthesized by the conventional sol-gel auto-combustion and their physical-chemical properties were characterized by XRD, FTIR, SEM, TPR and XPS. The XRD results indicated that copper-cobalt oxide appeared in a mixture form of  $\text{Cu}_{0.15}\text{Co}_{2.85}\text{O}_4$  spinel and CuO phases, whereas the cobalt oxide was shown in the pure form of  $\text{Co}_3\text{O}_4$  spinel. The FTIR approved the formation of the spinel structure in both samples. The SEM results showed that both oxides are as nanoparticles. Application of the same synthesis conditions for both samples led to samples with different purity being obtained. The results of temperature program reduction (TPR) revealed that Cu-Co nano oxide is more reducible at lower temperatures. The copper-cobalt oxide exhibited higher activity than the  $\text{Co}_3\text{O}_4$  in catalytic combustion of toluene, which is explained by its higher reducibility at the reaction conditions and by a possible synergistic effect between Cu-Co oxide and CuO particles.

---

### 1. Introduction

Environmental pollutants and volatile organic compounds of most environmental pollutants are a challenge in the 21<sup>st</sup> century [1]. These compounds are emitted by many sources such as: printing processes, petrochemical assembles and refinery sources.

Toluene is an aromatic type of volatile organic compound and can cause severe environmental hazards and be harmful to the health of human beings [1, 2]. Catalytic oxidation is an effective method and catalysis plays a major role in conversion of pollutants. Transition metal oxides are a suitable

replacement for noble metal catalysts [3,4]. It is well recognized that the mixed metal oxides present more superior activity than individual oxides. Spinel type mixed oxides generally show high thermal resistance and specific catalytic properties. Nanoscale spinel oxides have been pursued extensively in the last few years [5-9]. One of the suitable catalysts for combustion of hydrocarbons at low temperatures is cobalt oxide catalysts [4, 5]. Nano scale cobaltite was approved that presents high activity for aromatic VOCs such a toluene, as reported by Wyrwalski and co-workers [10]. Cobalt mixed oxides could be

---

\* Corresponding author: a.hosseini@urmia.ac.ir

promising for redox reactions, since cobalt ions can reach variable oxidation states. For example,  $\text{CuCo}_2\text{O}_4$  and  $\text{CoCr}_2\text{O}_4$  spinels showed high activity in CO and hydrocarbons oxidation [11].

In this work, two  $\text{Co}_3\text{O}_4$  and Cu-Co nano metal oxides were synthesized using the same method (the sol gel combustion) under the same conditions and the correlation between the properties and activity in oxidation of toluene was studied. The catalysts were characterized by XRD, FTIR, XPS, TPR and SEM.

## 2. Experimental

### 2.1. Catalyst preparation

The details of the sol gel combustion method, used in this paper have been described in literature [2, 12, 13]. All the chemicals were supplied by Merck Company. In the case of  $\text{Co}_3\text{O}_4$ ,  $\text{Co}(\text{NO}_3)_2 \cdot 6\text{H}_2\text{O}$  (0.01 mol) and citric acid monohydrate ( $\text{C}_6\text{H}_8\text{O}_7 \cdot \text{H}_2\text{O}$ ) (0.02 mol) were dissolved in 100 mL of distillate water. The heating of the solution transformed it into a gel and increased heat to 190 °C which lead to the formation of a black material. Then, the sample was calcined at 650 °C for 5 h to remove any carbonaceous residues and for the formation of the mixed-oxide phase.

For synthesis of Cu-Co mixed oxide,  $\text{Cu}(\text{NO}_3)_2 \cdot 3\text{H}_2\text{O}$  (99.5 %) and  $\text{Co}(\text{NO}_3)_2 \cdot 6\text{H}_2\text{O}$  (99 %) with the stoichiometric ratio Cu: Co = 1:2 and citric acid monohydrate ( $\text{C}_6\text{H}_8\text{O}_7 \cdot \text{H}_2\text{O}$  (99.5 %)) were dissolved in distillate water. Other steps were similar to those of  $\text{Co}_3\text{O}_4$  synthesis.

### 2.2. Catalyst characterization

The characterization of the samples by X-ray diffraction was done on a SIEMENS D5000 diffractometer. The infrared spectra of the samples were recorded with a Bruker 27 in

the range of 3900 to 400  $\text{cm}^{-1}$  with 4  $\text{cm}^{-1}$  resolution. The scanning electron microscope (model EQ-C1-1) was used to obtain the SEM images. The temperature programmed reduction profiles of the samples were obtained by Micromeritics Autochem 2910 Analyzer with a flow of a mixture of 10 vol %  $\text{H}_2$  in argon.

XP spectra were obtained with a VG Escalab 200R spectrometer equipped with a hemispherical electron analyzer (constant pass energy of 50 eV) and a Mg K $\alpha$  ( $h\nu = 1254.6$  eV) X-ray source.

### 2.3. Evaluation of Catalytic Performance

Catalytic studies were carried out at atmospheric pressure and different temperatures in a straight quartz fixed-bed reactor ( $l = 60$  cm, i.d. = 0.8 cm), placed inside an electric furnace. A loading of 200 mg of catalyst in powder form was placed into the reactor. The temperature was controlled by a thermocouple placed inside the catalyst bed. Before starting each run, catalysts were pre-treated with 10  $\text{mL min}^{-1}$  of pure nitrogen at 400 °C in order to eliminate the possible compounds adsorbed on the catalyst surface. After this pretreatment, the reactor was cooled to 100 °C, and the reaction vapor was introduced by passing the carrier gas (nitrogen) flow through a saturator containing toluene solvent. The inlet and outlet of the reactor were analyzed by a Shimadzu 2010 gas chromatograph. All experimental runs were taken under steady state conditions [14].

## 3. Results and discussion

In the synthesis of the catalysts, the concentration ratio of citric acid to nitrate was 0.5, which is the optimum ratio resulted from our previous studies [12, 13, 15]. The X-ray

patterns of the samples are shown in Fig.1.

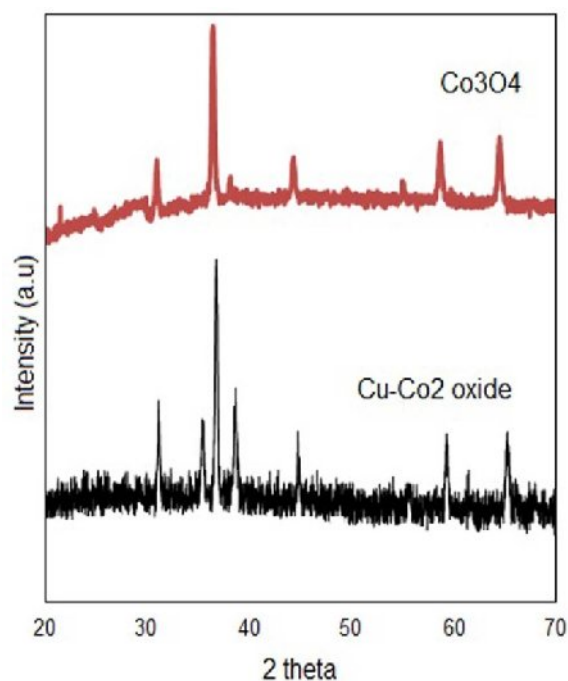


**Figure 1.** XRD pattern of Cu-Co<sub>2</sub> oxide and Co<sub>3</sub>O<sub>4</sub>.

The Cu-Co oxide presented a mixture of the corresponding spinel and some impurity of CuO. Thus, copper-cobaltite sample was in the form of a mixture of cubic Cu<sub>0.15</sub>Co<sub>2.84</sub>O<sub>4</sub> and some impurity of CuO (JCPDS 45-937) [11, 14]. The XRD patterns of cobaltite confirmed its appearance in Co<sub>3</sub>O<sub>4</sub> phase. Characteristic peaks of the samples have been shown in Fig.1. The peaks at  $2\theta$  of 31.3°, 36.8°, 44.8°, 59.3° and 65.2° correspond to reflection of (220), (311), (400), (511) and (440) for cubic Co<sub>3</sub>O<sub>4</sub> spinel (JCPDS 78-1970) [15-18]. The peaks of the sample obtained are slightly smaller than that of our previous cobaltite sample [16]. The prominent difference in the synthesis of these samples is the calcination temperature. In agreement with literature, the increase of calcination temperature increased the intensity of the peaks and consequently the crystallinity increased. According to Scherrer equation, the mean crystallite size of Cu-Co<sub>2</sub> and Co<sub>3</sub>O<sub>4</sub>

samples was determined to be 55 and 20 nm, respectively.

The infrared of spectroscopy of the Co<sub>3</sub>O<sub>4</sub> and CuCo<sub>2</sub>O<sub>4</sub> are shown in Fig.2.

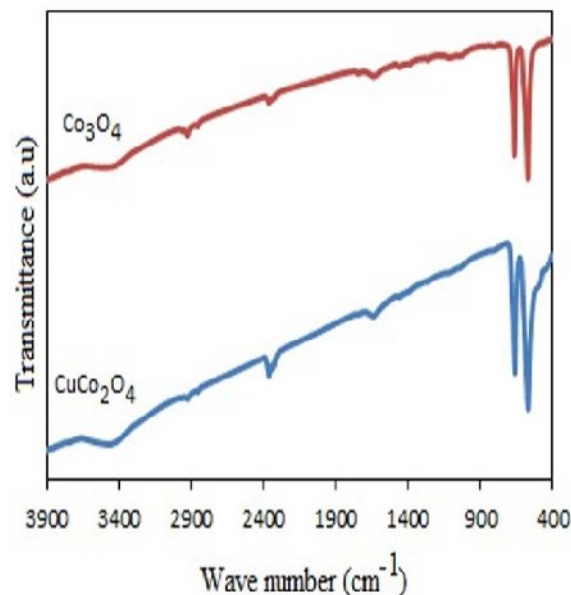


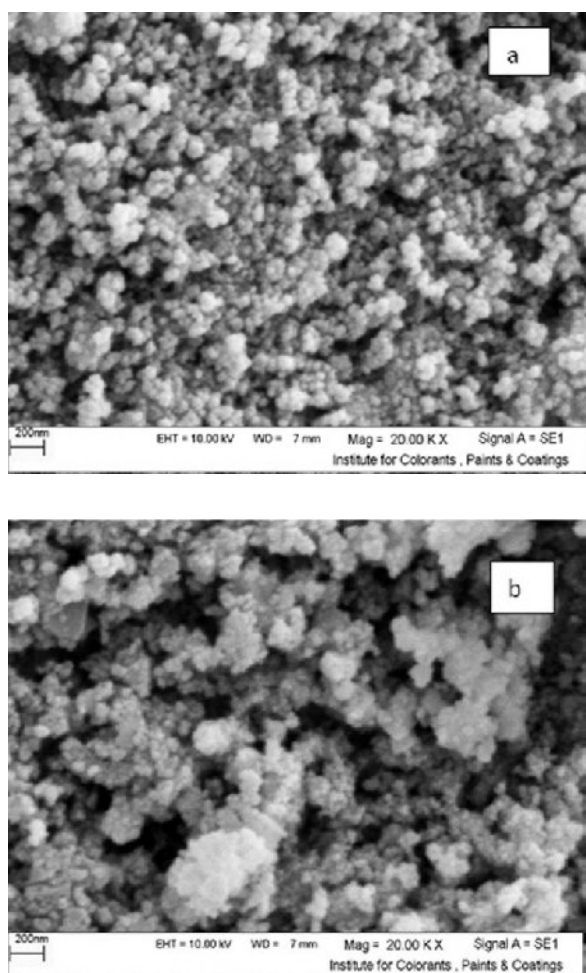
**Figure 2.** FTIR spectra of the catalysts.

Two bands are observed in the range 700 to 400 cm<sup>-1</sup>, corresponding to the stretching vibration of metal oxygen bonds [2]. For both spectra, the band around 500 and 600-700 cm<sup>-1</sup> corresponds to stretching band of Co-O in the tetrahedral system (T<sub>d</sub>) and stretching bond of Co-O in the octahedral system, respectively. The strong bands around 1620-1650 cm<sup>-1</sup> and 1322 cm<sup>-1</sup> are attributed to carboxylate and NO<sub>2</sub> functional groups, respectively [15, 19]. A broad band around 3300-3500 cm<sup>-1</sup> is ascribed to adsorption of water by KBr pellet [12-15].

For spectra of Cu-Co<sub>2</sub> oxide, the band at 500 cm<sup>-1</sup> corresponds to the stretching band of Cu-O in the tetrahedral system (T<sub>d</sub>). In the case of spectra of both samples, the band in the range 600-700 cm<sup>-1</sup> corresponds to the stretching bond of metal Co-O in the octahedral system [15].

The morphology and mean particle size of catalysts were investigated by SEM and the

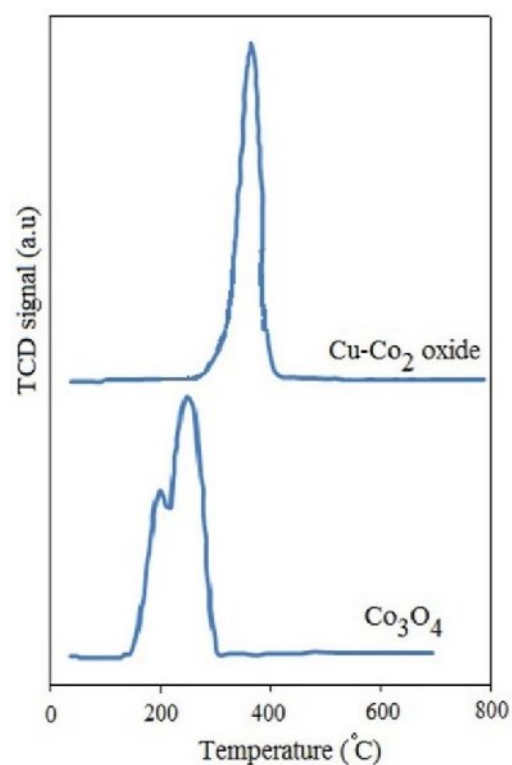
images are shown in Fig.3. Figure 3a shows that  $\text{Co}_3\text{O}_4$  particles are in the form of grain with a mean size of 40-70 nm [15]. The difference between the size resulted from XRD and SEM techniques is because XRD predicts the size of the crystallite, whereas the SEM shows the particle size. Thus, by consideration of the results of XRD and SEM it is suggested that each cobaltite particle contains 2-4 crystallites [15]. In the case of the SEM of  $\text{CuCo}_2\text{O}_4$ , the particles seem larger than those of  $\text{Co}_3\text{O}_4$  and some agglomeration of particles is seen in the Fig.3b.



**Figure 3.** SEM images of the catalysts.

The reducibility of fresh catalysts was determined using TPR profiles. Figure 4 shows the TPR profiles of the samples. A

reduction peak in TPR profile of  $\text{Co}_3\text{O}_4$  is ascribed to the reduction of cobaltite crystallites to  $\text{CoO}$  [20]. Two peaks around 195 and 240 °C are observed in TPR reduction profile of  $\text{Cu-Co}_2$  oxide. The lower temperature reduction peak is attributed to reduction of small particles of copper oxide to  $\text{Cu}^\circ$ , whereas the second peak can be attributed to the reduction of  $\text{Co}^{3+}$  in  $\text{CuCo}_2\text{O}_4$  spinel [11, 21].



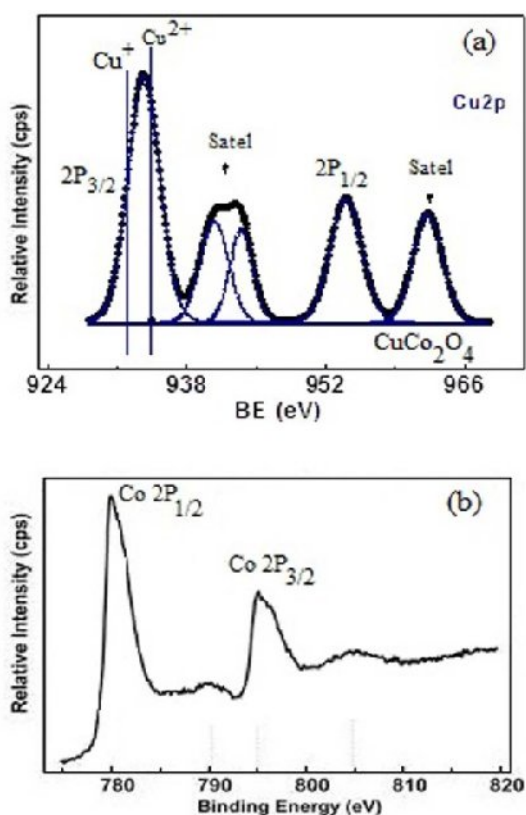
**Figure 4.** TPR profiles of the catalysts.

Figure 5 shows the XPS spectra of the catalysts. The atomic  $\text{Cu/Co}$  ratio was measured to be 0.43 for copper-cobalt oxide, which is in good agreement with the nominal ratio value 0.50, although some enrichment of  $\text{Co}$  element on the surface of the sample was observed. The  $\text{Cu } 2p$  spectra of  $\text{Cu-Co}_2$  oxide in Fig. 5(a) indicates two different signals. The signal at lower binding energy is due to  $\text{Cu(I)}$  and the signal with binding energies higher than 934 eV together with its satellite

between 940–945 eV is indicative of Cu(II) [11].

Figure 5b shows the XPS spectra of Co 2p spectrum of Cu-Co<sub>2</sub> oxide. The distinguishable satellite peaks appear at about 6 or 10 eV above the main line of Co 2p<sub>3/2</sub> (780 eV). These peaks are attributed to Co<sup>2+</sup> and Co<sup>3+</sup> species, in CoO and Co<sub>3</sub>O<sub>4</sub> in the surface Cu-Co sample, respectively.

In the case of XPS spectra of Co<sub>3</sub>O<sub>4</sub>, the shape and binding energies are similar to that reported for Co<sub>3</sub>O<sub>4</sub> spinel [11].



**Figure 5.** XPS spectra of the catalysts.

In order to compare the catalytic performance of the catalysts, the catalytic oxidation of toluene as a model molecule of aromatic VOCs was investigated.

Figure 6 shows the light-off curves for toluene oxidation over the catalysts.

The reaction temperature for fifty conversion of toluene (T<sub>50</sub> %) was considered as criteria

of catalyst activity, which is 249 and 225 °C for Co<sub>3</sub>O<sub>4</sub> and CuCo<sub>2</sub> nano oxides, respectively [11, 15]. This indicates that the activity of Cu-Co<sub>2</sub> nano oxide is more than that of Co<sub>3</sub>O<sub>4</sub> for oxidation of toluene. The result is in agreement with the results of Alizadeh et al. [22].

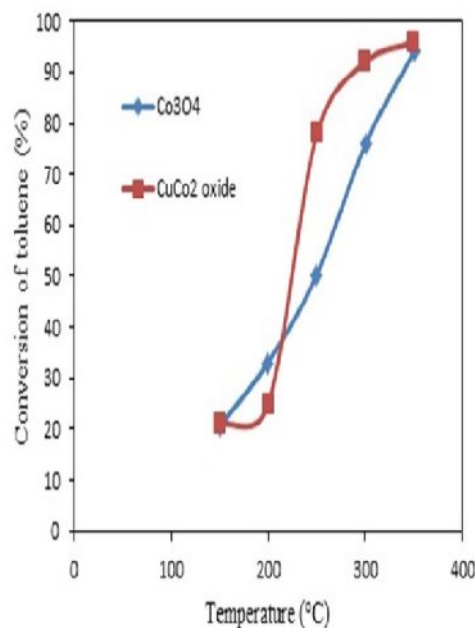


**Figure 6.** Light-off curves for catalytic conversion of toluene over catalysts.

Considering the TPR results and the activity of the nano metal oxides, it is resulted that there is a direct relationship between catalytic performance and reducibility. Since based on the TPR results, the Cu-Co nano oxide is able to be reduced more easily at lower temperature, it is more active at reaction temperatures. The better catalytic performance of Cu–Co nano oxide is also ascribed to a synergistic effect observed between Cu–Co spinel and a greater presence of CuO phase [21], due to enhanced electron transfer in these oxides [23, 24].

In the case of the mechanism of the oxidation on toluene on the catalysts, it is proposed that based on the Mars Van Krevelen (MVK) mechanism [1], the organic

molecule is oxidized by the surface oxygen on the oxide and the oxidation state of the cations is reduced. The reduced sites of the catalysts are then oxidized by gas phase oxygen.

#### 4. Conclusions

It is concluded that applying the same conditions for different nano metal oxides could lead to the samples with different purity being formed. The structural analysis by XRD approved that  $\text{CuCo}_2$  oxide is a mixture of spinel phase and  $\text{CuO}$ , whereas cobalt oxide appeared as pure  $\text{Co}_3\text{O}_4$  nano spinel. Obtained results show a relationship between the higher reducibility capability of the catalysts, based on  $\text{Cu-Co}_2$  oxide, and the higher activity for toluene combustion. The synergistic effect between  $\text{Cu-Co}$  spinel and  $\text{CuO}$  particles is also pointed out, supporting this reaction.

#### Acknowledgements

The author is grateful to Iranian Nanotechnology Initiative Council for the financial support. The author is also grateful to Professor Aligholi Niaei from the University of Tabriz for his assistance in the analysis of reaction products by GC.

#### References

- [1] Hosseini, S. A., Salari, D., Niaei, A. and Arefi Oskouei, S., "Physical-chemical property and activity evaluation of  $\text{LaB}_{0.5}\text{Co}_{0.5}\text{O}_3$  (B = Cr, Mn, Cu) and  $\text{LaMn}_x\text{Co}_{1-x}\text{O}_3$  (x = 0.1, 0.25, 0.5) nano perovskites in VOC combustion", *J. Ind. Eng. Chem.*, **19**, 1903 (2013).
- [2] Hosseini, S. A., Sadeghi, M. T., Alemi, A., Niaei, A., Salari, D. and Kafi Ahmadi, L., "Synthesis, characterization, and performance of  $\text{LaZn}_x\text{Fe}_{1-x}\text{O}_3$  perovskite nanocatalysts for toluene combustion", *Chin. J. Catal.*, **31**, 747 (2010).
- [3] Lou, X. W., Deng, D., Lee, J., Feng, J. and Archer, L., "Self-supported formation of needlelike  $\text{Co}_3\text{O}_4$  nanotubes and their application as lithium-ion battery electrodes", *Adv. Mater.*, **20**, 258 (2008).
- [4] Szegedi, A., Popova, A., Dimitrova, A., Cherkezova-Zheleva, Z. and Mitov, I., "Effect of the pretreatment conditions on the physico-chemical and catalytic properties of cobalt- and iron-containing Ti-MCM-41 materials", *Micropor. Mesopor. Mater.*, **136**, 106 (2010).
- [5] Konova, P., Stoyanova, M., Naydenov, A., Christoskova, St. and Mehandjiev, D., "Catalytic oxidation of VOCs and CO by ozone over alumina supported cobalt oxide", *Appl. Catal.: A.*, **298**, 109 (2006).
- [6] Song, O. and Zhang, Z. J., "Shape control and associated magnetic properties of spinel cobalt ferrite nanocrystals", *J. Am. Chem. Soc.*, **126**, 6164 (2004).
- [7] Sun, S. H. and Zeng, H., "Size-controlled synthesis of magnetite nanoparticles", *J. Am. Chem. Soc.*, **124**, 8204 (2002).
- [8] Zeng, H., Rice, P. M., Wang, S. X. and Sun, S. H., "Shape-controlled synthesis and shape-induced texture of  $\text{MnFe}_2\text{O}_4$  nanoparticles", *J. Am. Chem. Soc.*, **126**, 11458 (2004).
- [9] Sun, S. H., Zeng, H., Robinson, D. B., Raoux, S. P., Rice, M., Wang, S. X. and Li, G. X., "Monodisperse  $\text{MFe}_2\text{O}_4$  (M = Fe, Co, Mn) nanoparticles", *J. Am. Chem. Soc.*, **126**, 273(2004).
- [10] Wyrwalski, F., Lamonier, J. F., Perez-Zurita, M. J., Siffert, S. and Aboukar's, A., "Influence of the ethylenediamine addition on the activity, dispersion and reducibility of cobalt oxide catalysts

- supported over ZrO<sub>2</sub> for complete VOC oxidation”, *Catal. Lett.*, **108**, 87 (2006).
- [11] Hosseini, S. A., Niaei, A., Salari, D., Alvarez-Galvan, M. C. and Fierro, J. L. G., “Study of correlation between activity and structural properties of Cu-(Cr, Mn and Co)<sub>2</sub> nano mixed oxides in VOC combustion”, *Ceram. Int.*, **40**, 6157 (2014).
- [12] Hosseini, S. A., Alvarez-Galvan, M. C., Fierro, J. L. G., Niaei, A. and Salari, D., “MCr<sub>2</sub>O<sub>4</sub> (M=Co, Cu and Zn) nanospinel for 2-propanol combustion: Correlation of structural properties with catalytic performance and stability”, *Ceram. Int.*, **39**, 9253 (2013).
- [13] Hosseini, S. A. and Alvarez-Galvan, M. C., “Study of physical-chemical properties and catalytic activities of ZnCr<sub>2</sub>O<sub>4</sub> spinel nano oxides obtained from different methods - Modeling the synthesis process by response surface methodology and optimization by genetic algorithm”, *J. Taiwan Inst. Chem. Eng.*, **61**, 261 (2016).
- [14] Hosseini, S. A., Salari, D., Niaei, A., Deganello, F., Pantaleo, G. and Hojati, P., “Chemical-physical properties of spinel CoMn<sub>2</sub>O<sub>4</sub> nano-powders and catalytic activity in the 2-propanol and toluene combustion: Effect of the preparation method, Environ”, *Sci. Health, Part A.*, **46**, 291 (2011).
- [15] Hosseini, S. A., Niaei, A. and Salari, D., “Preparation and characterization of nano- and non-nanoscale Co<sub>3</sub>O<sub>4</sub> spinels obtained from different methods and study of their performance in combustion of aromatics from polluted air - A comparison with Pt/γ-Al<sub>2</sub>O<sub>3</sub> performance”, *Environ. Sci. Health, Part A.*, **47**, 1728 (2012).
- [16] Rivas, B., López-Fonseca, R., Jiménez-González, C., José, I. and Ortiz, G., “Synthesis, characterisation and catalytic performance of nanocrystalline Co<sub>3</sub>O<sub>4</sub> for gas-phase chlorinated VOC abatement”, *J. Catal.*, **281**, 88 (2011).
- [17] Shi, X., Han, S., Sanedrin, R. J., Zhou, F. and Selke, M., “Synthesis of cobalt oxide nanotubes from colloidal particles modified with a Co(III)-Cysteinato Precursor”, *Chem. Mater.*, **14**, 1897 (2002).
- [18] Zavyalova, U., Nigrovski, B., Pollok, K., Langenhorst, F., Müller, B., Scholz, P. and Ondruschka, B., “Gel-combustion synthesis of nanocrystalline spinel catalysts for VOCs elimination”, *Appl. Catal.: B.*, **83**, 221 (2008).
- [19] Solsona, B., Davies, T. E., Garcia, T., Va’zquez, I., Dejoz, A. and Taylor, S. H., “Total oxidation of propane using nanocrystalline cobalt oxide and supported cobalt oxide catalysts”, *Appl. Catal.: B.*, **84**, 176 (2008).
- [20] Chen, X., Zhang, J., Huang, Y., Tong, Z., and Huang, M., “Catalytic reduction of nitric oxide with carbon monoxide on copper-cobalt oxides supported on nano-titanium dioxide”, *J. Environ Sci.*, **21**, 1296 (2009).
- [21] Alizadeh-Gheshlaghi, E., Shaabania, B., Khodayaric, A., Azizian-Kalandaraghd Y. and Rahimi, R., “Investigation of the catalytic activity of nano-sized CuO, Co<sub>3</sub>O<sub>4</sub> and CuCo<sub>2</sub>O<sub>4</sub> powders on thermal decomposition of ammonium perchlorate”, *Powder Technol.*, **217**, 330 (2012).
- [22] Tang, Q., Wu, C., Qiao, R., Chen Y. and Yang, Y., “Catalytic performances of Mn-Ni mixed hydroxide catalysts in liquid-phase benzyl alcohol oxidation

- using molecular oxygen”, *Appl. Catal. A.*, **403**, 136 (2011).
- [23] Vodyankin, A., Kurina L. and Popov, V., “Multicomponent oxide catalysts of a deep oxidation of carbon monoxide”, *Kinet. Catal.*, **40**, 636 (1999).
- [24] Chen, M. and Zheng, X., “The effect of K and Al over NiCo<sub>2</sub>O<sub>4</sub> catalyst on its character and catalytic oxidation of VOCs”, *J. Mol. Catal.: A.*, **221**, 77, (2004).